Catalysis Today 213 (2013) 73–80

Contents lists available at SciVerse ScienceDirect

Catalysis Today

journal homepage: www.elsevier.com/locate/cattod

Investigation of the stability of Novozym® 435 in the production of biodiesel

Carla José[a], Gregory B. Austic[b], Rita D. Bonetto[a], Rachel M. Burton[b], Laura E. Briand[a,*]

[a] Centro de Investigación y Desarrollo en Ciencias Aplicadas-Dr. Jorge J. Ronco (CINDECA), Universidad Nacional de La Plata, CONICET, CCT La Plata, Calle 47 Nº 257, B1900AJK La Plata, Buenos Aires, Argentina
[b] Piedmont Biofuels 220 Lorax Lane, Pittsboro, NC, USA

ARTICLE INFO

Article history:
Received 26 November 2012
Received in revised form 21 January 2013
Accepted 11 February 2013
Available online 30 March 2013

Keywords:
Novozym® 435
Biodiesel
FAeSTER
Enzymatic esterification

ABSTRACT

The effect of the composition of the feedstock (free fatty acids and methanol), the presence or absence of moisture and the contact with biodiesel on the catalytic, enzymatic and physical stability of Novozym® 435 during enzymatic biodiesel production was studied. The continuous removal of moisture leads to the deactivation of the biocatalyst and favours the degradation of the polymethylmethacrylate (PMMA) that constitutes the support of the lipase B of *Candida antarctica* (CALB). Nevertheless, the presence of PMMA along with the active protein was detected in the reaction media regardless of the operating conditions. Surprisingly, biodiesel (without the presence of methanol) is able to diffuse inside the biocatalyst's beads producing its swelling, modifying the internal texture and also dissolving the polymeric matrix.

1. Introduction

Novozym® 435 is the commercial immobilized *Candida antarctica* lipase B (CALB) produced by submerged fermentation of a genetically modified *Aspergillus* microorganism. The lipase is adsorbed on a macroporous resin called Lewatit VP OC 1600, according to the information given by the Novozymes Co. in their website. This macroporous resin is a polymer of metacrylic acid cross-linked with divinylbenzene (DVB) and possesses certain hydrophobic nature [1]. Recently, some of us demonstrated that both neat ethanol and an ethanol: H_2O mixture dissolve the polymethylmethacrylate (PMMA) that constitutes the support of the lipase B of *Candida antarctica* (CALB) regardless of the conditions investigated and also diffuses into the biocatalyst's beads remaining strongly adsorbed (the desorption of the alcohol was evidenced only upon heating at 150 °C) [2]. Our research demonstrated that 16.6% of the initial mass of biocatalyst was dissolved upon contacting Novozym® 435 with ethanol (or ethanol–water mixture) for 4 cycles of 48 h at 45 °C. The action of ethanol over the integrity of the PMMA resin was also determined on the inner texture of the biocatalyst's beads. In fact, the microscopic analysis of the cross section of the beads demonstrated the increase of their roughness and internal pore structure. Additionally, the ethanol (with or without water added) modifies the secondary structure of the enzyme by decreasing the α-helix contributions and increasing the β-sheet structure. The conclusions obtained in those investigations evidence that the deactivation reported by ourselves and other researchers on the catalytic activity of Novozym® 435 in contact with alcohols cannot be explained straightforwardly since there is a multiplicity of effects that account for such phenomena. In this context, a similar methodology was applied to investigate the stability of Novozym® 435 in the biodiesel production under various operation conditions. As it is already well known, biodiesel fuel is produce by esterification of fatty acids or transesterification of oils and fats with short chain, low cost alcohols that are currently supplied as a commodity material [3]. Although, methanol causes severe drawbacks such as reaction inhibition and a lower enzyme performance, it is currently the alcohol most widely used in biodiesel production [4]. Now, reviewing those investigations devoted to the enzymatic biodiesel production comes clear that the alcohol to oil molar ratio influences enzyme life and is the key parameter in enzyme screening for biodiesel production. Although, many scientific publications proved that the catalytic performance of both free and immobilized lipases (Novozym® 435) is severely affected by methanol, none of them addresses the causes of such inhibition [3–6]. These investigations focused on how to override the inhibition rather than to explain why inhibition occurs and what the consequences are on the quality of the product. The present investigation provides relevant information concerning the effect of free fatty acid to methanol ratio, the presence of moisture and the contact with biodiesel on the catalytic, enzymatic and

* Corresponding author. Tel.: +54 221 4 211353/210711.
E-mail address: briand@quimica.unlp.edu.ar (L.E. Briand).

0920-5861/$ – see front matter © 2013 Elsevier B.V. All rights reserved.
http://dx.doi.org/10.1016/j.cattod.2013.02.013

physical stability of Novozym® 435 during enzymatic biodiesel production. In this context, the modifications of the outer and inner texture of the biocatalyst, its physical integrity (loss of polymeric support and/or the enzyme in the reaction media) and the effect on the enzyme's secondary structure were investigated.

2. Experimental

2.1. Transesterification of free fatty acids toward biodiesel

Two samples of 0.2 g of Novozym® 435 (batch #LC200229) were reused 92 (sample called #218 along the article) and 117 times (sample called #219) respectively in the esterification of free fatty acids (called FFA for brevity) toward biodiesel at 65 °C for 2 h. Each reuse was the reaction of 44 ml of a mixture containing 4.2% FFA oleic acid with 0.46% of methanol added at the beginning of the reaction. The sample #218 had continuous moisture removal through the FAeSTER process while the sample #219 did not [7]. After the reaction and 1 min of settling, 15 ml of the reaction media was taken from each reaction and filtered through 2.5 μm filter paper. After 30 min of additional settling, an additional 15 ml of liquid was filtered through 2.5 μm filter paper. The 30 min sample is to help identify how much of the particulate is suspended such that it cannot be removed by gravity.

A third sample of Novozym® 435 called #220 was used once in the esterification of 15% FFA soy and oleic acid with 1.58 wt% of methanol added at start of reaction.

Additionally, a sample of Novozym® 435 was tested in a pilot scale reactor (called "*pilot*" sample from now on) for 2 h reaction time (single use), at a temperature of 65 °C, sparged agitation, with 4% FAME (fatty acids methyl esters) and 0.23 ml methyl alcohol. The pilot scale multi-catalyst biodiesel reactor possesses a stainless steel batch reaction tank (132.5 l), with continuous glycerol removal, oil and biodiesel purification.

Novozym® 435 saturated in biodiesel for 4 h was used as a reference sample (called "*control*" sample from now on). The biodiesel was the commercial product of Piedmont Biofuels that typically contains <0.08% FFA and <0.05% methanol in accordance with ASTM specifications [8].

2.2. Procedure for the treatment of the beads of Novozym® 435

The samples of Novozym@ 435 called *control*, #218, #219 and the one used in the pilot plant were washed with tert-butanol (Sigma–Aldrich 99.0%) in order to remove the residues of FFA and biodiesel adsorbed on the beads. The samples were washed three times with about ~1 ml of the alcohol in the container and then were filtered with a conventional filter paper. The biocatalysts' beads were also washed with distilled water in order to remove the alcohol that crystallizes at room temperature. The beads were allowed to dry in a desiccator at room temperature.

2.3. Analysis of the material retained on the filter papers

Each filter was weighed and then washed with anhydrous ethanol (Carlo Erba, HPLC grade) for 25 min at room temperature in order to remove the retained material. The filters were dried and reweighed after being washed. The remaining alcohol after washing was evaporated leaving an oily layer residue with a small particulate matter embedded in it. This material was weighed and then dissolved in 8.00 ml of ethanol and filtered through nylon filters of 0.45 μm (Osmonics). Then these nylon filters were dried, weighed and the material held on them was analyzed by FTIR. On the other hand, the liquid phase was carried to dryness and the resulting residue was weighed and dissolved in 1.00 ml of distilled water. The aqueous phase was centrifuged for 10 min at 14,000 rpm in a Spectrafuge 16M Labnet centrifuge in order to separate the aqueous layer from the remaining oily layer. The aqueous layer was further analyzed through UV–Vis spectroscopy with a Perkin Elmer Lambda35 spectrophotometer in order to determine the presence of protein as described in previous studies [2]. The amount of protein was further determined through the bicinchoninic acid assay as will be discussed in the following section.

2.4. Quantification of the protein through the bicinchoninic acid assay

The amount of protein that was recovered from the reaction media was quantified through the bicinchoninic acid assay. The BCA method involves the preparation of three aqueous solutions that are called A, B and C for brevity. Solution A contains 0.4000 g of BCA (Fluka ≥ 90%), 0.8000 g Na_2CO_3 (Mallinckrodt), 0.1630 g $NaHCO_3$ (Anedra), 0.1581 g NaOH (Carlo Erba ≥ 97%) and 0.0641 g sodium tartrate dibasic dihydrate (Fluka ≥ 99%) in 40 ml of distilled water. Solution B contains 4% (w/v) of $CuSO_4$ and solution C is a mixture of solution A and B in a 100/2 (v/v) ratio (in this particular case, solution C corresponds to 30.00 ml of solution A and 0.60 ml of solution B, and is prepared just before the quantification).

The standard solutions for the calibration curves were prepared with *Candida antarctica* lipase (CALB L) (batch LCN02102) containing 68.30 mg/ml of protein. This concentration was determined previously through the precipitation of the protein [2]. That starting aqueous solution of CALB L was further diluted to 0.1 mg/ml and the standard solutions for calibration purposes were prepared by taking an appropriate volume of the 0.1 mg/ml of the CALB L solution then 2.00 ml of the solution C was added and incubated at 60 °C for 10 min (each solution was prepared by duplicate). The mixtures were allowed to cool down and the absorbance was measured at 562 nm (the spectrophotometer was described in Section 2.3). The calibration curves were performed in an interval containing from 2.25 μg/ml to 9.01 μg/ml.

2.5. Determination of the secondary structure of the protein with infrared spectroscopy

The secondary structure of the biocatalyst was determined through infrared analysis. The samples were diluted with KBr and pressed in a conventional wafer for FTIR analysis. Spectra were collected in the 4000–400 cm^{-1} range (±2 cm^{-1} resolution) with a Bruker Vertex 70 equipment. The infrared analysis was recorded with 120 scans in the absorption mode. The contribution of the infrared spectrum of the support Lewatit VP OC1600 was digitally subtracted from the spectra of Novozym® 435. Similarly maximum absorption intensity of all the spectra was verified, which indicates that a constant optical path length was maintained during the analysis of the samples.

To estimate the secondary structure, peak fitting of the Amide I band (1700–1600 cm^{-1}) by Lorentzian-shaped components was performed on the non-deconvoluted spectra. The software used with this purpose was a special peak fitting module of Origin 5.0. The positions and number of the components were determined from the second derivative analysis of the spectra. The contribution of each component to the Amide I band was evaluated by integrating the area under the curve and then normalizing to the total area of the Amide I band.

2.6. Scanning electron microscopy analysis and description of the inner and outer texture

The diameter of the beads along with the inner and outer morphology of the starting Novozym® 435, soaked in biodiesel (control

sample) and after reaction was investigated through scanning electron microscopy analysis with a Philips SEM 505. The samples were prepared as thin specimens by embedding the biocatalyst in a LR White resin and further sliced with a microtome. This procedure allowed obtaining samples of the cross sections of the beads for the investigation of the inner texture. These specimens, covered with a conductive gold layer in order to avoid electrical charges on the surface, were observed in the microscope. Images of the cross section of the samples at a magnification equal to 8400× (25 kV, spot size 20) were analyzed with the FERImage program in order to calculate the fractal dimension D, d_{per} and the d_{min} parameters [21]. The capabilities of such software are discussed in the following sections.

3. Results and discussion

3.1. Life trials of Novozym® 435 in the production of biodiesel

Fig. 1 shows the catalytic performance of two samples of Novozym® 435 tested in the esterification of a feedstock containing 4% of (FFA) with 0.46% of methanol with and without continuous removal of moisture (these samples are called #218 and #219, respectively). Additionally, the figure shows the esterification of a feedstock containing 15% FFA with 1.58% of methanol without moisture removal (sample called #220). The data corresponds to the percentage of non converted FFA that remains in the batch after 120 min versus enzyme productivity calculated as the amount of biodiesel produced (in Ton.) per kilogram of biocatalyst. The outlier data points correspond to result from testing at 40 and 80 min time.

The set of data points belongs to 92 consecutives runs performed with the sample #218 and 117 batches that were run with both samples #219 and #220. The sample #218 suffers the most noticeable activity loss since the amount of FFA remaining in the reaction media goes up continuously (less ester production) from the 83rd batch. The moisture levels were consistently less than 100 ppm along the experiments, therefore high moisture does not account for the activity loss. Additionally, the reaction media shows more fine particulates than the other samples. These fine

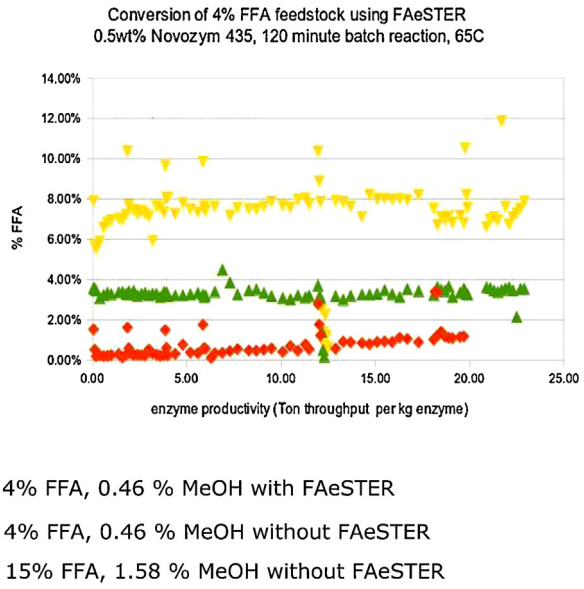

Fig. 1. Life trials of Novozym® 435 through several reuses of the biocatalyst in the esterification of feed stocks containing 4% FFA (with and without FAeSTER) and 15% FFA (without FAeSTER) at 65 °C for 120 min of reaction. The graph shows the percentage of FFA remaining in the reaction media versus de enzyme productivity in tons per kg of enzyme.

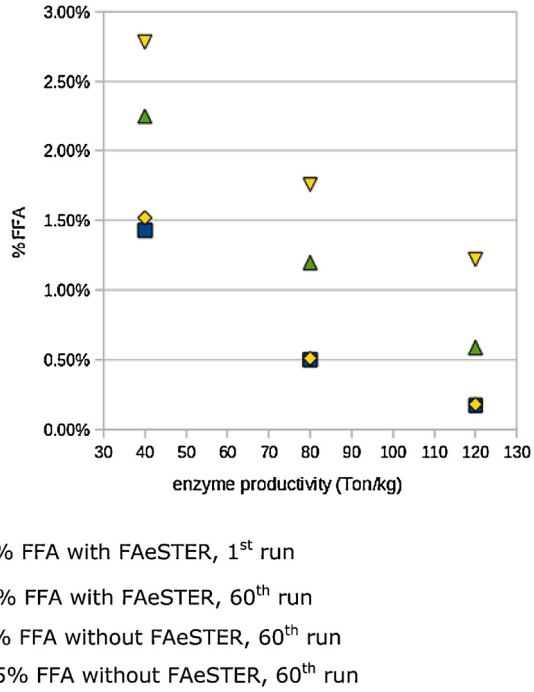

Fig. 2. Comparison of the catalytic performance of three samples of Novozym® 435 used 60 times and further reacted (two batches of 120 min each) with moisture removal (FAeSTER method). The graph shows the percentage of FFA remaining in the reaction media versus de enzyme productivity in tons per kg of enzyme.

particulate whose nature is discussed in the following sections, remain in suspension for extended periods of time.

In order to achieve a comparable measurement of deactivation for all samples, each of them were reacted using the FAeSTER method with the same conditions after the 60th batch. In this context, the samples #219 and #220 were rinsed with 30 ml of fresh 4% FFA biodiesel before reacting in order to remove any left-over oil or water. The sample #220 was reacted twice with 4% FFA using the FAeSTER method (120 min each batch) in order to ensure that the results were not affected by the presence of water from previous batches containing 15% FFA. Fig. 2 shows the percentage of non converted FFA that remains in the reaction media versus enzyme productivity under continuous moisture removal through the FAeSTER method.

The results corresponding to the first run of 120 min of reaction carried with a feedstock containing 4% FFA using the FAeSTER method shows a high substrate conversion toward biodiesel. However, the biocatalyst previously used 60 times and then reacted with the FAeSTER method evidences deactivation comparing with the non moisture removal operation. It is worth noticing that the catalytic activity of Novozym® 435 remains stable when moisture is not removed from the reaction media (compare 4% FFA no FaeSTER runs 1 and 60 in Fig. 2).

The reaction performed with 15% FFA without moisture removal show a similar performance compared with the 4% FFA containing feedstock at about 120 min of operation. Again, the results evidence that the presence of moisture plays an important role in the catalytic stability of Novozym® 435.

3.2. Evidences of the degradation of Novozym® 435 in the reaction media

The results described in the previous section clearly evidence the deactivation of Novozym® 435 under several reuses when moisture is removed from the reaction media. In this context, the physical and enzymatic stability of the biocatalyst was further

Table 1
Amount of solid residue and protein found in the reaction media due to the degradation of Novozym@ 435 during the production of biodiesel with and without moisture removal through the FAeSTER method.

Novozym® 435	Time of collection[a]	(w/v) % of residues[b]				(w/v) % protein (mg/100 ml)
		Biodiesel + PMMA + enzyme + others	Non soluble residue (PMMA)[c]	Water soluble residue	Non soluble in water or ethanol (fats, biodiesel)	
# 218 with FAeSTER	1 min	1.36	1.28	–	0.08	11.58
	30 min	1.19	0.15	0.90	0.14	11.01
# 218 without FAeSTER	1 min	1.39	0.10	1.11	0.18	8.68
	30 min	1.36	0.35	0.86	0.15	8.82
# 219 with FAeSTER	1 min	1.31	0.11	1.08	0.12	10.76
	30 min	1.49	0.16	1.14	0.19	9.04
# 219 without FAeSTER	1 min	1.35	0.13	1.08	0.14	15.08
	30 min	1.47	0.22	1.05	0.20	9.27

[a] The sample of the reaction media was collected after 1 min and 30 min of the ending of the reaction.
[b] The (w/v) % of solid residue was determined in 15.00 ml of the liquid medium and extrapolated to 100 ml.
[c] These values correspond to the subtraction of the amount of soluble and non soluble residues to the total amount of residues.

evaluated in order to obtain fundamental insights that allow correlating the catalytic performance and the intrinsic properties of the biocatalyst.

First of all the reaction media was investigated in order to determine if any of the constitutive materials of the biocatalyst (protein and/or polymethylmethacrylate) were left in the liquid media after reaction. As a second approach the biocatalyst's beads were assayed in order to establish the modification of the texture and/or the secondary structure of the protein.

The reaction media was filtered after reaction and the presence of the particulate and/or the enzymatic material was investigated after removal of the biodiesel as previously described in Section 2.3. Table 1 presents the amount of residue per volume that was recovered from the reaction media after 1 min and 30 min of the ending of the reaction along with the content of protein. As expected, the reaction media evidences the presence of an oily component (non soluble either in water or ethanol, not retained by a 0.45 μm filter). However, aside from this component there are two other ones: a non soluble solid residue that is suitable to be retained by a 0.45 μm filter and a water soluble residue. Interestingly, the higher amount of the non soluble solid residue (1.28 w/v %) belongs to the sample #218 that was used with continuous water removal and finally deactivates upon reuses. This non soluble residue corresponds to the polymeric matrix of the beads of biocatalyst as will be discussed in the following section.

The UV–Vis analysis of the water soluble residue evidences the presence of characteristic signals of the components of Novozym® 435 such as a broad and intense signal ascribed to benzoic acid (230 nm) and sorbic acid (258 nm) used as preservatives in the manufacture of Novozym® 435 (spectra not shown). Additionally, a shoulder observed at 282 nm corresponds to the absorbance of peptide bonds and amino acids containing aromatic rings, respectively. More evidences of the presence of proteins were obtained through the quantification with the bicinchoninic acid assay that indicates a concentration of about 0.4–0.7 mg/ml of protein in the reaction media regardless of the operative conditions (see Table 1).

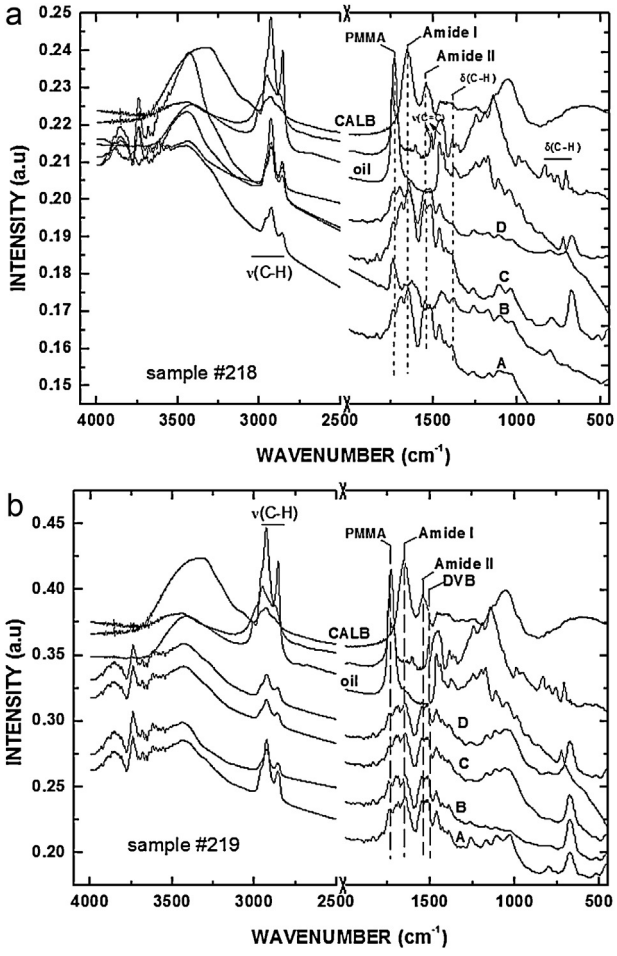

Fig. 3. (a) Infrared spectra of *Candida antarctica B*, bare support Lewatit VP OC 1600 of polymethylmethacrylate PMMA, oil residue and residues of the reaction media after using the sample #218. These spectra correspond to the following operation conditions: (A) and (B) without FaeSTER filtered after 1 min and 30 min after the ending of operation; (C) and (D) with FaeSTER filtered after 1 min and 30 min after the ending of operation. (b) Infrared spectra of *Candida antarctica* B, bare support Lewatit VP OC1600 of polymethylmethacrylate PMMA, oil residue and residues of the reaction media after using the sample #219. These spectra correspond to the following operating conditions: (A) and (B) without FaeSTER filtered after 1 min and 30 min after the ending of operation; (C) and (D) with FaeSTER filtered after 1 min and 30 min after the ending of operation.

3.3. Evidences of the loss of the polymeric matrix of Novozym® 435

The nature of the residues recovered from the reaction media was determined through infrared spectroscopy as will be discussed in this section. Fig. 3a and b shows the infrared spectra of the solid particulate recovered from the filters along with the infrared spectra of the oil recovered from the biocatalyst's beads after washing with tert-butanol, the polymeric support polymethylmethacrylate

PMMA and the lipase B of *Candida antarctica*. Additionally, Table 2 summarizes the band's position and the assignments of the infrared signals.

The bare support Lewatit VP OC 1600 possesses an intense signal at 1731 cm^{-1} due to the stretching vibration of the carbonyl groups of the polymethylmethacrylate PMMA $-(CH_2CCH_3)_n-CO-O-CH_3$ [9,10]. Additionally, the intense signals belonging to asymmetric and symmetric stretching of the methyl groups (2950 cm^{-1} and 2875 cm^{-1}, respectively) along with asymmetric and symmetric bending vibrations (of weak intensity) of the methyl groups (1387 cm^{-1} and 1361 cm^{-1}, respectively) are observed [11]. These last two signals are characteristic of the C—H vibration of methyl and methylene groups attached to a tertiary carbon atom such as the one of the PMMA resin. The intense set of signals observed in the range from 1269 cm^{-1} to 1145 cm^{-1} are characteristic of twisting and wagging vibrations of methylene groups. The presence of divinylbenzene as a cross-linker is evidenced through the doublet of medium intensity at 1510 cm^{-1} and 1454 cm^{-1} due to the skeletal vibrations involving the carbon–carbon stretching within the aromatic ring. Additionally, a set of weak signals is observed from 834 cm^{-1} to 709 cm^{-1} that is characteristic of the C—H out-of-plane bending bands of the alkyl-substituted benzene [10,11].

The oily residue possesses two intense bands at 1742 cm^{-1} and 1713 cm^{-1} ascribed to the stretching vibration of the carbonyl species ν(C=O) of the ester linkage COOR that belongs to either the free fatty acids or the biodiesel [12–14]. Additionally, the stretching vibrations of CH_3, CH_2 and CH appear at 3002 cm^{-1}, 2928 cm^{-1} and 2858 cm^{-1} along with the bending vibrations of the methylene groups $(CH_2)n$ of the long chains at 1463–1350 cm^{-1}, 1350–1150 cm^{-1} and 724 cm^{-1}.

The infrared spectra of the lipase B of *Candida antarctica* possesses the intense bands corresponding to the Amide I and Amide II signals centered at 1653 cm^{-1} and 1540 cm^{-1}, respectively [15,16]. These signals are observed in the residues recovered from the reaction media providing further evidences of the loss of protein from Novozym® 435 during the production of biodiesel.

The overlapping between the infrared signals of the carbonyl group (~1730 cm^{-1}) of FFA, biodiesel and PMMA makes difficult to analyze the presence of the polymeric matrix in that region. However, the residues possess the signal of divinylbenzene at about 1510 cm^{-1} that is the cross-linker of the polymeric matrix as discussed before (the signal at 1463 cm^{-1} might also belongs either to DVB or to the oily residue). Further evidences is provided by the signal of medium intensity at 674 cm^{-1} that is ascribed to the out of plane bending of the carbon–hydrogen bonds δ(C=C—H) of aromatic substances [2,10].

3.4. Effect of the reaction conditions on enzyme's secondary structure

Fig. 4 shows the infrared spectra of the starting Novozym® 435, control, #218 (reused 92 times), #219 (reused 117 times) and the one used in the pilot plant. The commercial biocatalyst Novozym® 435 possesses both the signals belonging to the lipase B of *Candida antarctica* (a weak signal belonging to Amide I is observed at about 1651 cm^{-1}) and the macroporous polymer as expected. In this context it is interesting to compare the ratio of the areas of the infrared signals belonging to PMMA versus the Amide I as a semi-quantitative evidence of the alteration of the content of the support and the active enzyme. The "control" biocatalyst that was just soaked in biodiesel, the samples that were reused several times in the biodiesel production process and the sample used once in the pilot plant possess lower ratios than the starting sample indicating a certain degree of alteration of both the content of protein and polymeric matrix (see Table 3). The biocatalyst used once in the pilot plant possess the closer ratio compared with the starting

Table 2
Summary of the nature of the organic groups and the corresponding infrared signals that were detected on Novozym® 435, Lewatit VPOC, *Candida antarctica* CALB lipase, the oil residue and the solids recovered from the reaction media.

	ν(O—H)	ν(C—N)	ν(CH_3)	ν(C=O)	Amide I	Amide II	Aromatic ring vibration ν(C=C)	δ_{as}(C—H)	δ_s(C—H)	ν_{as}(C—O)	ω(CH_2) τ(CH_2)[a]	Out-of-plane δ(C—H)[b]	δ(CH_2)n
CALB lipase		3331 cm^{-1}	2928 cm^{-1}		1653 cm^{-1}	1540 cm^{-1}							
Lewatit VPOC	3436 cm^{-1}		2950 cm^{-1}; 2875 cm^{-1}	1731 cm^{-1}			1510 cm^{-1}; 1454 cm^{-1}	1387 cm^{-1}	1361 cm^{-1}		1269–1145 cm^{-1}	991, 969(s), 834, 800, 757,709 cm^{-1}	
Oil residue	3417 cm^{-1}		3002 cm^{-1}; 2928 cm^{-1}; 2858 cm^{-1}	1742 cm^{-1}; 1713 cm^{-1}				1463–1350 cm^{-1}	1350–1150 cm^{-1}	1300–1000 cm^{-1}			724 cm^{-1}
Recovered solids	3437 cm^{-1}		2958 cm^{-1}; 2857 cm^{-1}	1741 cm^{-1}; 1692 cm^{-1}	1646 cm^{-1}	1552 cm^{-1}	1510 cm^{-1}; 1463 cm^{-1}	1384 cm^{-1}		1259–1039 cm^{-1}		674 cm^{-1}	

[a] ω(CH_2) and τ(CH_2) wagging and twisting vibration of methylene groups.
[b] Out of plane bending of the aromatic C—H groups.

Table 3
Ratio between the areas of the infrared signals of the polymeric support PMMA at 1735 cm^{-1} and the protein at 1651 cm^{-1}, and contribution of the individual components of the secondary structure of Novozym® 435.

Novozym® 435	A_{1731}/A_{1651} [a]	Percentage contribution %				
		β-Aggregates	α-Helix	Random	β-Sheet[b]	β-Turn[c]
Starting sample	5.9	–	26.4	20.5	21.8	31.3
Control	2.8	0.7	13.6	16.8	56.2	12.7
#218	1.8	4.8	25.4	15.9	39.7	14.2
#219	2.2	2.6	12.7	15.8	45.6	23.3
Pilot	4.0	4.0	23.0	17.1	36.3	19.2

[a] A_{1731} and A_{1651} correspond to the areas of the infrared signals centered at 1731 cm^{-1} and 1651 cm^{-1} ascribed to PMMA resin and Amide I, respectively.
[b] The percentage of (-sheet corresponds to the addition of the contribution of the most intense signals at 1631 cm^{-1}, 1641 cm^{-1} and 1695 cm^{-1}.
[c] The percentage of (-turn corresponds to the addition of the contribution of the signals at 1667 cm^{-1}, 1678 cm^{-1} and 1680 cm^{-1}.

Novozym® 435 ($A_{PMMA}/A_{Amide\ I}$ = 4.0 versus 5.9) while the reused samples #218 and #219 present the lower ratios of the investigated series. This observation suggests that the longer the reaction the higher the degradation of the biocatalyst's beads. Moreover, being the area of the infrared signal of the polymeric matrix A_{PMMA} higher than the area of the signal of the protein A_{AmideI} allows concluding that the content of polymethylmethacrylate decreases at a higher rate than the protein content upon reusing.

Interestingly, the sample that was just soaked in biodiesel (no subjected to reaction) also shows a certain degree of degradation compared with the fresh biocatalyst (A_{PMMA}/A_{AmideI} = 2.8 versus 5.9 of the starting biocatalyst). Additionally, the secondary structure of the lipase B of *Candida antarctica* was also affected upon contacting with the biodiesel. In this context, the analysis of the infrared spectra of enzymes in the 1700–1600 cm^{-1} region (the so-called Amide I region) provides qualitative and also quantitative information of the secondary structure elements that compose the protein [2,15,16]. The Amide I band originates from the stretching vibrations of the peptide carbonyl groups in the backbone of the protein, whose frequency depends on the hydrogen-bonding and coupling along the protein chain, and is therefore sensitive to the protein conformation. The Amide I signal of the infrared spectra of the starting Novozym® 435, the control, #218, #219 and the sample used in the pilot plant were de-convoluted in order to obtain evidences of the secondary structure changes of the proteins. In this context, Table 3 shows the percentage contribution of the different elements of the secondary structure. As was discussed above, even the exposure to the biodiesel at room temperature alters the secondary structure of the *Candida antarctica* lipase increasing the β-sheet structure and decreasing the contributions of the α-helix and β-turn structures compared with the starting Novozym® 435. The samples used in the reaction show a similar behavior although in the particular cases of the sample #218 and the one used in the pilot plant do not alter their α-helix structure. It is worth noticing that the control and the used Novozym® 435 possess β-aggregates which are an indication of misfolding followed by aggregation of the protein. This phenomenon is produced when the protein is subjected to stress perturbation such as thermal treatment, pH variations and high salt concentrations [17,18].

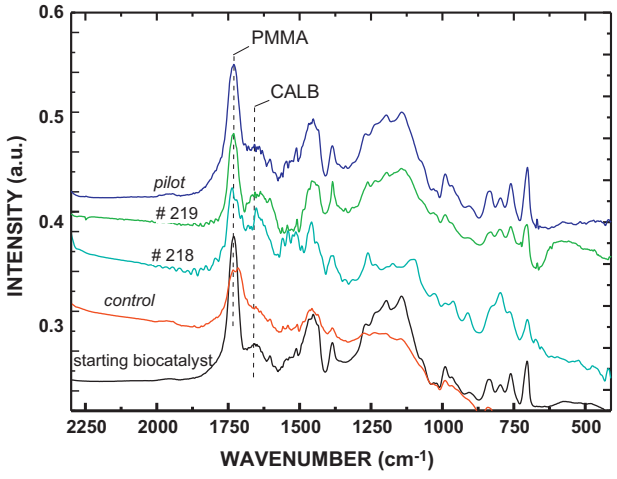

Fig. 4. Infrared spectra of the beads of starting Novozym® 435, after being in contact with biodiesel (*control* sample); used in a pilot plant and reused 92 times (sample #218) and 117 times (sample #219) in the esterification of a FFA feedstock.

3.5. Modification of the external and internal texture of biocatalyst

Fig. 5a–e is micrographs of the beads of the starting Novozym® 435, the control, #218, #219 and the sample used once in the pilot plant, respectively. The analysis of the diameter of several beads of each sample indicates an interesting variation going from an average of 539 μm for the starting biocatalyst, 626 μm for the sample soaked in biodiesel, 478 μm for the sample #218 (reused 92 times under reaction conditions), 427 μm for the sample #219 (reused 117 times) and 612 μm for the sample used once in the pilot plant (see Table 4). The biocatalyst's beads soaked in biodiesel at room temperature (without reaction) possessed a higher diameter than the starting material which clearly evidenced the swelling of the beads. This observation correlates with previous investigations reported by Heinsman and col. and ourselves [2,19,20]. The former researchers demonstrated that a typical free fatty acid such as, 4-methyloctanoic acid and its ester (4-methyl octanoic acid ethyl ester) diffuse and adsorb (7.2 ± 2.6 mmol of fatty acid per gram of enzyme) into Novozym® 435 causing a 175–250% increase in the bead's volume. Surprisingly, this phenomenon happens in just 2 min after the beads were soaked in the substrates at room temperature.

Additionally, the images of the cross section of the samples at a magnification of 8400× were taken with the Philips SEM 505 and analyzed with the FERImage program to calculate the fractal dimension D, d_{per} and d_{min} parameters by using the variogram method. The variogram, used to determine a series of parameters that characterize the surface roughness, consists of a graph of the variance of variation of heights in a surface for different steps, as a function of such steps at logarithmic scale [21–24]. The slope of the graph is related to the fractal dimension D as D 3 – slope/2. The d_{min} parameter characterizes the roughness of the samples and is representative of the smallest cell size with enough statistic weight to produce periods. Additionally, the parameter d_{per} is a measurement of the average diameter of "holes" among these nearest elementary cells ("virtual circles" representatives of regions that separate these cells) [24].

In this context, five images corresponding to five different particles for each case were studied and their average values of D, d_{per} and d_{min} along with their uncertainties are reported in Table 4. The contact with biodiesel and the reaction conditions modify the

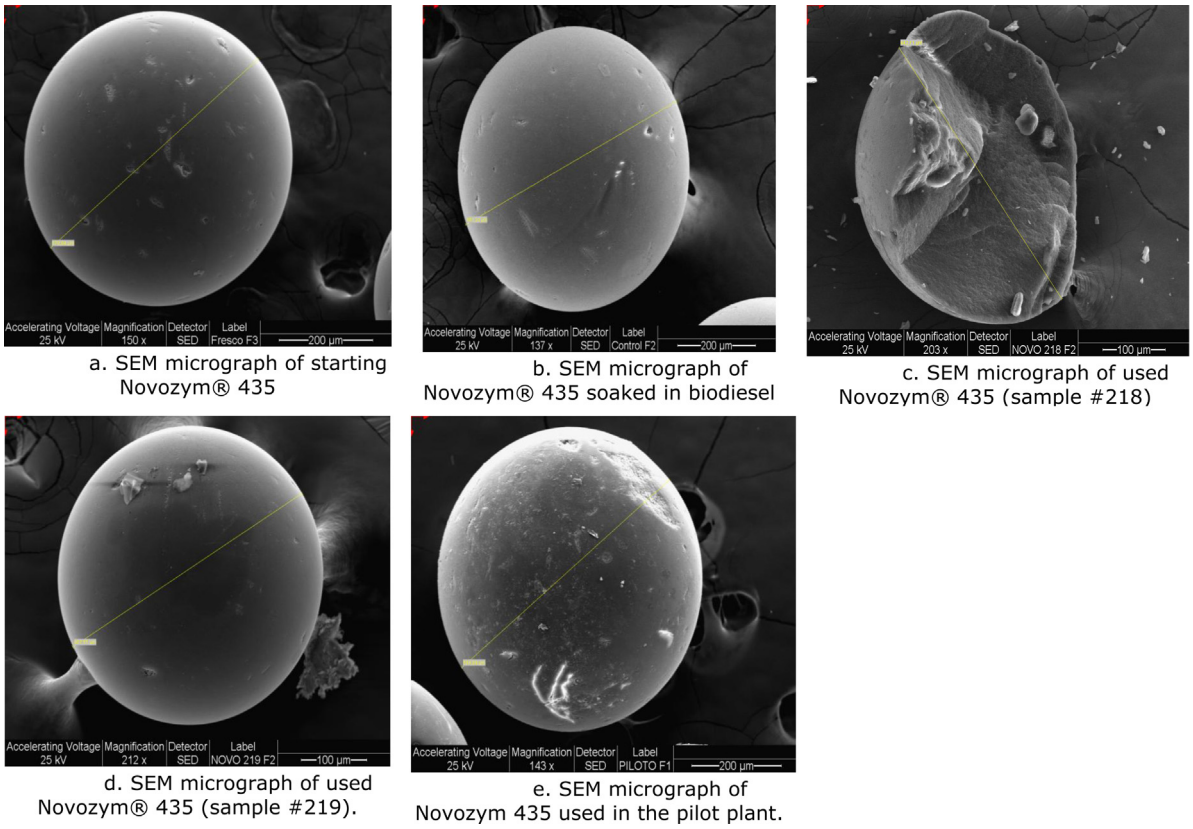

Fig. 5. Micrographs of the beads of Novozym® 435: (a) starting biocatalyst; (b) after being in contact with biodiesel; (c) reused 92 times (sample #218); (d) reused 117 times (sample #219) and (e) used in the pilot plant for the esterification of a FFA feedstock toward biodiesel.

Table 4
Average diameter of the biocatalyst's beads, fractal dimensions D, minimum cell size d_{min} with enough statistic weight to produce periods and d_{per}, the distance within such elementary cells.

Novozym® 435	Diameter[a] (μm)	d_{min} [a] (μm)	d_{per} [a] (μm)	D[a]
Starting sample	539	0.129 ± 0.014	1.766 ± 0.015	2.593 ± 0.010
Control	626	0.1066 ± 0.0026	1.111 ± 0.070	2.417 ± 0.010
#218	478	0.114 ± 0.040	1.12 ± 0.30	2.525 ± 0.068
#219	427	0.1009 ± 0.0045	1.05 ± 0.12	2.642 ± 0.034
Pilot	612	0.1113 ± 0.0058	1.59 ± 0.10	2.638 ± 0.011

[a] The values given in the Table are an average of at least five different samples of the biocatalyst.

texture with opposite trends. In this context, the *control* sample shows a lower D value than the starting sample while the samples #218, #219 and *pilot* possess higher D values than Novozym® 435. In this context, the sample #219 that was reused more times than the #218 also presents the more significant modification of its internal texture.

The modification of the texture correlates with the decrease of the d_{min} of the sample #219 that again possesses the lower value of the assayed materials. Additionally, the d_{per} parameter decreases reaching similar values for the samples #218, #219 and *control*.

4. Conclusions

The present investigation demonstrates that the catalytic stability of Novozym® 435 in the esterification of free fatty acids is not affected by the ratio of FFA to methanol or even the source of such free fatty acids but to the presence of moisture. In this context, the deactivation of the biocatalyst cannot be explained straightforward since there is a multiplicity of effects that account for such phenomena. For one side, the biodiesel diffuses inside the biocatalyst's beads and produces its swelling. Similarly, the investigation of some of us evidences such phenomena upon contacting the biocatalyst's beads with ethanol, ethanol–water, 2-propanol–water mixtures at room temperature for at least 40 min [2,25]. Earlier investigations reported by Lee demonstrated that also methanol penetrates PMMA beads [26]. The authors observed that the penetration of methanol in PMMA beads possesses an induction period followed by an extended region of linear front penetration toward the center. The induction period decreases whereas the front velocity increases with increasing temperature going from 25 °C toward 50 °C. Since the esterification of FFA with methanol in the present investigation is carried at 65 °C is expected that the alcohol diffuses rapidly inside the biocatalyst's beads affecting the integrity of the polymer.

Additionally, several investigations evidence that polymethylmethacrylate PMMA is dissolved by mixtures of solvent pairs such as ethanol/water, acetonitrile/alcohol and water/alcohol (methanol, 2-propanol, ethanol and 1-propanol), CCl_4/alcohols, benzyl alcohol/sec-butyl chloride between others [26–29]. Particularly, Hoogenboom et al. investigated the solubility of PMMA in various aqueous-alcohol solutions and they correlated the solubility of the polymer to the hydration of the polymer chains due to the

hydrogen bonding of water molecules to the PMMA ester groups [29]. The authors demonstrated that only a slightly improved solubility of PMMA is observed upon addition of water to methanol, which is most likely due to the hydration of the ester groups. In fact PMMA dissolves in aqueous solution containing from 70 wt.% to 100 wt.% of methanol at temperatures ranging from about 50 °C to 70 °C. Those observations correlate with the fact that PMMA (non-soluble residue) was found in the reaction media regardless of the application of the FAeSTER method for moisture removal. The alteration of the secondary structure of the lipase B of *Candida antarctica* (the active enzyme) under moisture free operation might be an additional cause of deactivation. In fact, the protein possesses a higher contribution of β-aggregates after reaction without water than the one reacted under the presence of moisture.

Acknowledgments

The authors acknowledge Mariela Theiller for technical supports in the acquisition of SEM images and the financial support of CONICET (project PIP 0083) and Universidad Nacional de La Plata (project 2012–2015).

References

[1] A. Ganesan, B.D. Moore, S.M. Kelly, N.C. Price, O.J. Rolinski, D.J.S. Birch, I.R. Dunkin, P.J. Halling, ChemPhysChem Special Issue: Biophysics 10 (2009) 1492–1499.
[2] C. José, R.D. Bonetto, L.A. Gambaro, M. del Pilar Guauque Torres, M.L. Foresti, M.L. Ferreira, L.E. Briand, Journal of Molecular Catalysis B-Enzymatic 71 (2011) 95–107.
[3] T. Tan, J. Lu, K. Nie, L. Deng, F. Wang, Biotechnology Advances 28 (2010) 628–634.
[4] L. Fjerbaek, K.V. Christensen, B. Norddahl, Biotechnology and Bioengineering 102 (2009) 1298–1315.
[5] C-C. Lai, S. Zullaikah, S.R. Vali, Yi-H. Ju, Journal of Chemical Technology and Biotechnology 80 (2005) 331–337.
[6] H.-M. Chang, H.-F. Liao, C.-C. Lee, C.-J. Shieh, Journal of Chemical Technology and Biotechnology 80 (2005) 307–312.
[7] FAeSTER stands for fatty acid esterification using enzymes under continuous water removal developed by Piedmont Biofuels (patent pending).
[8] ASTM D6751-11b standard specification for biodiesel fuel blend stock (B100) for middle distillate fuels.
[9] Y. Mei, L. Miller, W. Gao, R.A. Gross, Biomacromolecules 4 (2003) 70–74.
[10] R.M. Silverstein, G.C. Bassler, T.S. Morrill, Spectrometric Identification of Organic Compounds, J. Wiley & Sons, 1991, pp. 102–131.
[11] Infrared spectra database of the National Institute of Standards and Technology (http://webbook.nist.gov) of methyl acrylate $C_4H_6O_2$ (CAS: 96-33-3) and m-divinyl benzene C10H10 (CAS: 108-57-6).
[12] L.F. Bezerra de Lira, M.S. de Albuquerque, J.G. Andrade Pacheco, T.M. Fonseca, E.H. de Siqueira Cavalcanti, L. Stragevitch, M.F. Pimentel, Microchemical Journal 92 (2010) 126–131.
[13] M. Tariq, S. Ali, F. Ahmad, M. Ahmad, M. Zafar, N. Fhalid, M.A. Khan, Fuel Processing Technology 92 (2011) 336–341.
[14] O.M. Martinez Avila, F.J. Sánchez Castellanos, O.Y. Suárez Palacios, Revista Ingeniería e Investigación 27 (2007) 34–43.
[15] A. Barth, Biochimica et Biophysica Acta 2007 (1767) 1073–1101.
[16] M.L. Foresti, G.M. Valle, R.D. Bonetto, M.L. Ferreira, L.E. Briand, Applied Surface Science 256 (2010) 1624–1635.
[17] A. Natalello, R. Santarella, S.M. Doglia, A. de Marco, Protein Expression and Purification 58 (2008) 356–361.
[18] J. Kardos, K. Okuno, T. Kawai, Y. Hagihara, N. Yumoto, T. Kitagawa, P. Závodszky, H. Naiki, Y. Goto, Biochimica et Biophysica Acta 1753 (2005) 108–120.
[19] N.W.J.T. Heinsman, C.G.P.H. Schroën, A. van der Padt, M.C.R. Franssen, R.M. Boom, K. van't Riet, Tetrahedron: Asymmetry 14 (2003) 2699–2704.
[20] C. José, L.E. Briand, Reac Kinetics, Mechanism and Catalysis 99 (1) (2010) 17–22.
[21] F.D. Bianchi, R.D. Bonetto, Scanning 23 (2001) 193–197.
[22] J.L. Ladaga, R.B. Bonetto, in: Peter W. Hawkes (Ed.), Characterization of Texture in Scanning Electron Microscope Images. Advances in Imaging and Electron Physics, vol. 120, Academic Press, Unites States, 2002, pp. 136–189, ISSN: 1076-5670-02.
[23] A.P. Pentland, IEEE Transactions on Pattern Analysis and Machine Intelligence (TPAMI) (6) (1984) 661–674.
[24] R.D. Bonetto, J.L. Ladaga, Scanning 20 (1998) 457–463.
[25] M.V. Toledo, C. José, S.E. Collins, R.D. Bonetto, M.L. Ferreira, L.E. Briand, Journal of Molecular Catalysis B-Enzymatic 83 (2012) 108–119.
[26] P.I. Lee, Polymer 34 (11) (1993) 2397–2400.
[27] J.M.G. Cowie, M.A. Mohsin, I.J. McEwen, Polymer 28 (1987) 1569–1572.
[28] J. González-Benito, J.L. Koenig, Polymer 47 (2006) 3065–3072.
[29] R. Hoogenboom, C.R. Becer, C. Guerrero-Sanchez, S. Hoeppener, U.S. Schubert, Australian Journal of Chemistry 63 (2010) 1173–1178.